

## TEST RESULTS OF $b=0.64$ , 700 MHZ, 5-CELL ELLIPTICAL CAVITIES\*

T. Tajima<sup>†</sup>, K. C. D. Chan, R. L. Edwards, R. C. Gentzlinger, W. B. Haynes, J. P. Kelley, F. L. Krawczyk, J. E. Ledford, M. A. Madrid, D. I. Montoya, D. L. Schrage, A. H. Shapiro, Los Alamos National Laboratory, Los Alamos, NM 87545, USA; J. Mammoser, TJNAF, Newport News, Virginia, USA

### Abstract

Six 5-cell superconducting elliptical cavities have been fabricated at LANL and in industry and tested at LANL and TJNAF. The APT (Accelerator Production of Tritium) specification requires  $Q_0 > 5 \times 10^9$  at an accelerating field of 5 MV/m. So far, the results of vertical tests have shown maximum accelerating fields of 12 MV/m (peak surface field of 41 MV/m and 835 Oe) and maximum  $Q_0$  of  $3.6 \times 10^{10}$  at 2 K ( $2.1 \times 10^{10}$  at  $E_{acc} = 5$  MV/m). The present limitations are available input power, field emission and quench. With a new 600 W amplifier and a mapping system for surface temperature and x-ray radiation, we are trying to identify and localize the emission/quench source(s) to further improve the cavity performance.

### 1 INTRODUCTION

The APT accelerator, if it is built, is a 100-mA, 1.7-GeV CW proton linac [1]. A number of papers have been published on the development of APT superconducting cavities, power couplers and cryostats in the past [2]. Since APT was named as a backup option to the commercial light-water reactor program in December 1998 [3], the ED&D activities shrank significantly. Tests, however, of all the six 700-MHz 5-cell cavities manufactured as part of prototyping efforts have been performed in vertical cryostats at LANL and TJNAF (Thomas Jefferson National Accelerator Facility). This paper presents the results of these tests in more detail as well as some future plans.

### 2 CAVITIES

Table 1 shows the names, niobium suppliers, manufacturers and the initial thickness of the niobium of all the cavities. The LANL cavity was made in house at LANL. AES stands for Advanced Energy Systems, an American company. The last four cavities were manufactured by CERCA, a French company, and the cavities were named after popular female names of the countries where niobium suppliers are located.

Table 2 shows the parameters of the cavities [7]. The CERCA cavities were manufactured after LANL and AES cavities and their parameters are slightly different due to the increase in radius of the end beam pipe from 6.5 cm to

8 cm. This modification was made to obtain sufficient coupling between power coupler and beam [6].

The cavities are made of RRR=250 niobium and their inner surfaces were chemically etched 150  $\mu$ m at the manufacturers. Figure 1 shows a cavity installed in the cryostat insert.

Table 1: List of all the APT Prototype Cavities

Cavity Name	Nb Supplier	Manufacturer	Nb Thickness
LANL	Teledyne Wah Chang	LANL	3.175 mm
AES	Wah Chang	AES	3.5 mm
Ayako	Tokyo Den kai	CERCA	4 mm
Eleanore	Wah Chang	CERCA	4 mm
Germaine	Heraeus	CERCA	4 mm
Sylvia	Wah Chang	CERCA	4 mm

Table 2: Parameters of APT 5-cell Cavities

Frequency	700 MHz
$\beta$	0.64
R/Q	392(374) $\Omega$
Geometrical Factor	149 $\Omega$
$E_p/E_{acc}$	3.381 (3.272)
$H_p/E_{acc}$	69.6(68.6) Oe/MV/m

Note: the values in the parentheses are for LANL and AES cavities.



Figure 1: APT 5-cell cavity set on the cryostat insert.

\* Work supported by the US Department of Energy

<sup>†</sup> email: tajima@lanl.gov

### 3 SURFACE TREATMENT AND PREPARATION AT LANL

After delivery to LANL, the cavities were chemically etched again with a standard BCP (Buffered Chemical Polishing) solution of 1:1:2 [4]. Then, they were rinsed with high-pressure de-ionized water at ~950 psi in a class-100 clean room and assembled with couplers, flanges and a vacuum valve. Once sealed in the clean room, the cavity was moved to a measurement room, set on the cryostat insert, and pumped down and leak checked. Before cooled down, the cavities were baked at 150 °C for 48 hours. It should be noted that no cavities were baked at temperatures higher than this before testing.

### 4 TEST RESULTS

Figure 2 shows the Q-E curves of all the cavities. The tests conducted at TJNAF are marked as JLAB with the legend. The data for Eleanore cavity between 4 MV/m and 11.5 MV/m are missing since we could not take the

final data due to damage to the driving coupler cable. As for the LANL cavity, there were difficulties in performing the final equator weld in the middle cell and we found the  $Q_0$  drop shown in Fig. 2 was caused by some defect at this equator from heating detected by a temperature sensor. Before the LANL cavity was tested in January 2001, low-field  $Q_0$  obtained at LANL were lower than those recorded at TJNAF. We have investigated the cause of these differences as written in Section 5.3.

#### 4.1 Limitations

At LANL, the available RF power was limited to ~250 W. Degradation of  $Q_0$  due to field emission limited performance, although it appeared that most of the cavities would have quenched at fields slightly higher than their maximum fields due to heating at defects or heating by electron bombardment on the surface. At TJNAF, however, they stopped measurement of the AES cavity so as not to damage the driving coupler cable. Germaine and Sylvia cavities were limited by quench.

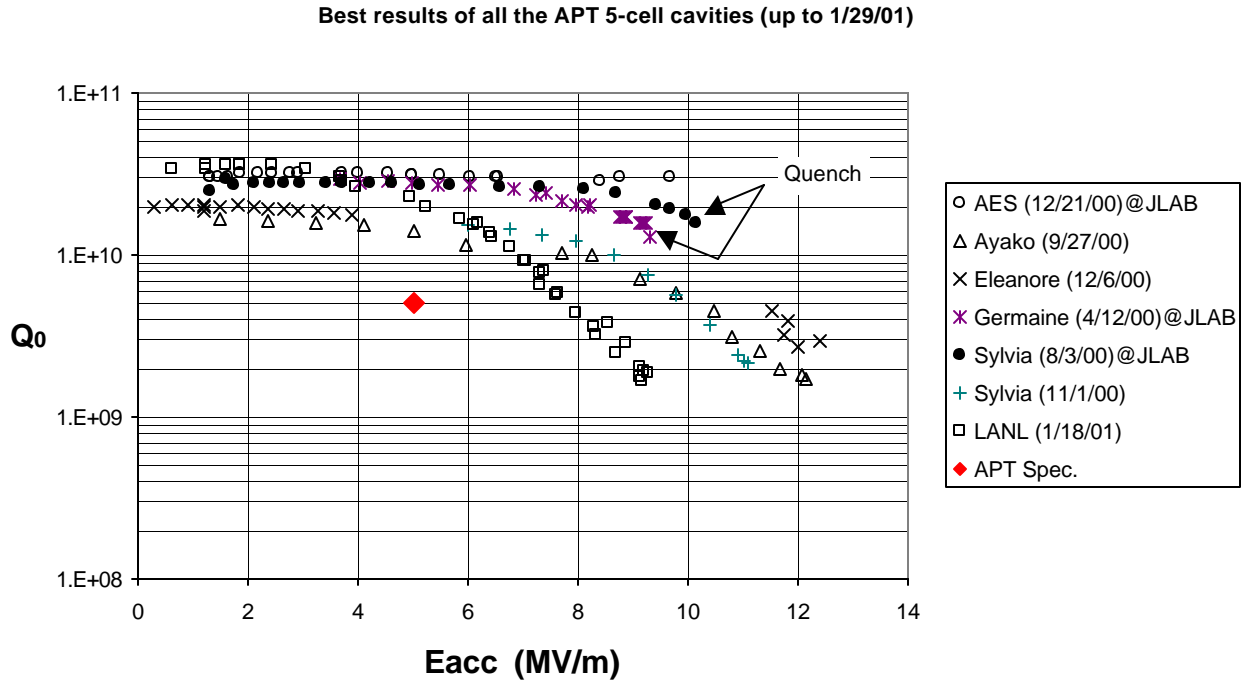


Figure 2: Test results of all six 5-cell cavities developed for APT. All the tests were performed in vertical cryostats at 2 K. In this figure only the best results are shown. The factors that contributed to these results are discussed in the text. The results obtained at TJNAF are depicted as @JLAB in the legend.

### 5 DISCUSSION

The results shown in Fig. 2 are the best results for each cavity. Most cavities needed either further chemical etching, and/or RF processing and/or helium processing, although processing did not take more than a few hours. These effects will be discussed below.

#### 5.1 Effect of Further Chemical Polishing

The inner surfaces of all the cavities were chemically etched 150  $\mu\text{m}$  with a solution of nitric, hydrofluoric and phosphoric acid in a volumetric ratio of 1:1:2 in industry after manufacturing. Our initial plan calls for ~20  $\mu\text{m}$  of final etching before performance test in a vertical cryostat. However, most of the cavities did not show good results

with this amount of etching. For example, the Ayako cavity did not show good results after first and second BCP, but after another 60  $\mu\text{m}$  of etching improved the performance significantly as shown in Fig. 3. In our experience, further BCP of  $>60 \mu\text{m}$  always helped improve the performance.

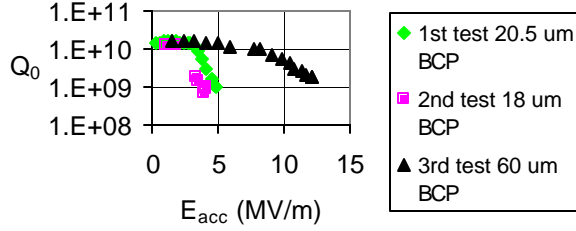


Figure 3: Effect of further etching with Ayako cavity.

### 5.2 Effect of Helium Processing

Helium processing is one of the oldest methods employed to improve cavity performance. It helped us improve some of our cavities as well. For example, the Eleanore cavity suffered heavy field emission, but with helium processing it could reach over 10 MV/m as shown in Fig. 4. A disadvantage of helium processing is that  $Q_0$

decreases slightly after helium processing and it tends to degrade after the next thermal cycle, although it can be recovered with another helium processing in most cases.

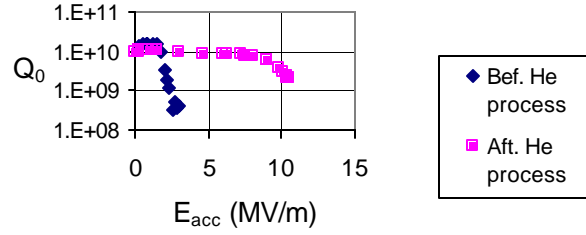


Figure 4: Effect of helium processing with Eleanore cavity.

Figure 5 shows a combination of both further etching/polishing and helium processing. Further polishing followed by high-pressure rinsing sometimes increases the  $Q_0$  as shown in Fig. 5. As shown in Fig. 2, we could improve the performance so that all the cavities exceed the APT requirements by either further BCP, helium processing or a combination of them.

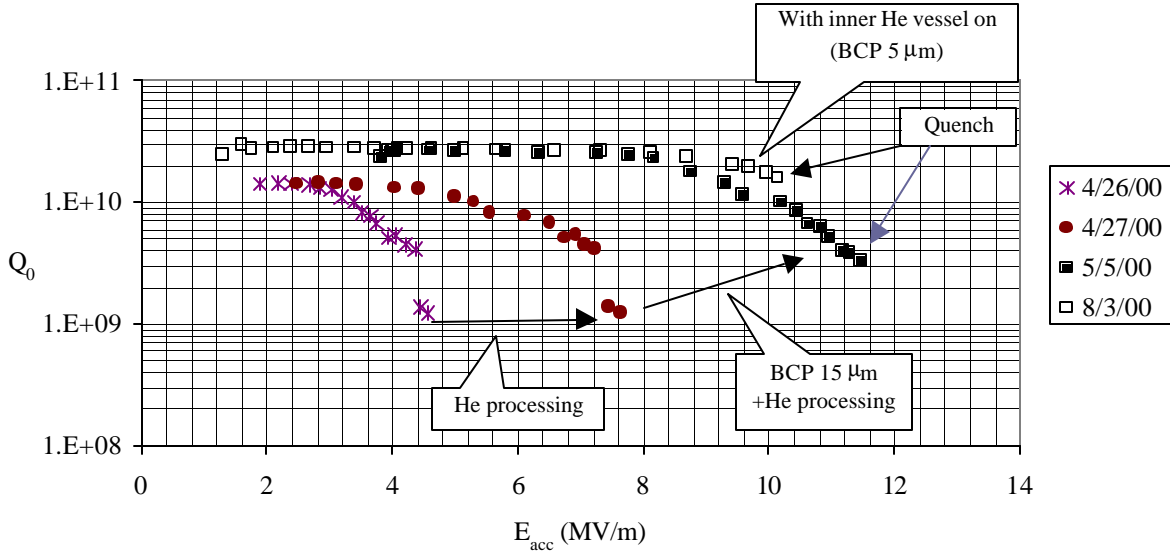


Figure 5: Effect of a mixture of helium processing and further BCP. Also shown is the data after welding of inner helium vessel. This data is of Sylvia cavity.

### 5.3 Factors Affecting Low-Field $Q_0$ values

In all of the tests conducted at LANL in 2000, low-field  $Q_0$  values were  $< \sim 2 \times 10^{10}$  as compared to  $\sim 3 \times 10^{10}$  obtained at TJNAF.

Since  $Q_0 = G/R_s$ , where  $G$  and  $R_s$  are the geometrical factor and the surface resistance, respectively, the higher the surface resistance, the lower the  $Q_0$ . In the case of APT 5-cell cavities, using

$G = 149 \Omega$  from Table 2, the surface resistances for  $Q_0 = 2 \times 10^{10}$  and  $3 \times 10^{10}$  are  $7.5 \text{ n}\Omega$  and  $5.0 \text{ n}\Omega$ , respectively, i.e., the difference of the surface resistance is  $2.5 \text{ n}\Omega$ .

Surface resistance is expressed as  $R_s = R_{\text{BCS}} + R_{\text{res}}$ , where  $R_{\text{BCS}}$  and  $R_{\text{res}}$  are the BCS resistance and the residual resistance, respectively. As for BCS resistance, it is theoretically expressed as follows [8].

$$R_{BCS} = A \cdot f^2 \cdot 1/T \cdot \exp[-B/T],$$

where A and B are constants dependent on the material properties of the superconductor, f the frequency and T the surface temperature.

For our 700 MHz cavities at 2 K, experimentally obtained  $R_{BCS}$  was 1.7 n $\Omega$ . If the temperature varies from 1.9 K to 2.1 K (this is our normal variation),  $R_{BCS}$  varies from 1.1 n $\Omega$  to 2.6 n $\Omega$ , i.e., if the measurement temperatures at LANL and TJNAF are different by 0.2 K, it would lead to a difference of 1.5 n $\Omega$ . Thus, we concluded this alone did not explain the difference.

As for  $R_{es}$ , we considered the effect of ambient magnetic field in the cryostat. We measured the ambient magnetic fields in the vertical cryostats at both LANL and TJNAF.

Figure 6 shows the results on normal measurement conditions, i.e., field compensation coil is on. It was found that the magnetic field at TJNAF is about 2 mG lower than that at LANL. Also, the magnetic field near the top cell starts rising at LANL as shown in Fig. 6.

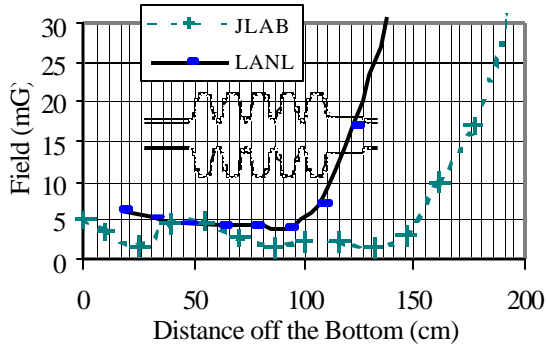


Figure 6: Ambient magnetic field in the vertical cryostats at LANL and TJNAF.

To know the dependence of  $Q_0$  on the magnetic field values, we took  $Q_0$ - $E_{pk}$  curves at various ambient magnetic fields as shown in Fig. 7.

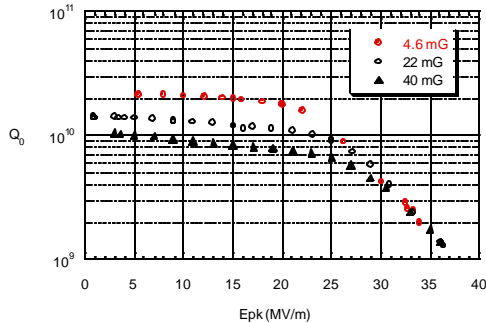


Figure 7:  $Q_0 - E_{pk}$  curves of Sylvia cavity taken at various magnetic fields before cooling. Magnetic fields are an average of 5 cells.

Figure 8 shows the surface resistance calculated from low-field  $Q_0$  values as a function of ambient magnetic

fields. The surface resistance increased linearly at 0.22 n $\Omega$ /mG. This result indicates that the contribution of the difference of ambient magnetic fields between LANL and TJNAF is about 0.44 n $\Omega$  since the difference is 2 mG. Also, as one can see in Fig. 8, the surface resistance gets only 6 n $\Omega$  even if we try to make the ambient magnetic field zero, implying that reduction of ambient magnetic field alone will not raise the  $Q_0$  to  $3 \times 10^{10}$  or  $R_s = 5$  n $\Omega$ . Thus, we concluded that the difference of ambient magnetic fields alone could not explain the difference of 2.5 n $\Omega$ .

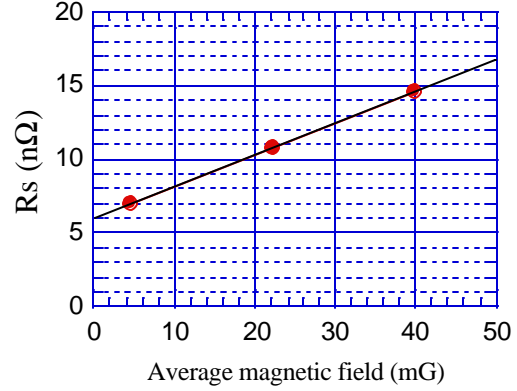


Figure 8: Residual resistance as a function of magnetic field averaged over 5 cells. The sensitivity is calculated to be 0.22 n $\Omega$ /mG.

In January 2001, when we tested LANL cavity, we obtained a low-field  $Q_0$  of  $3.6 \times 10^{10}$ . What we did for the LANL cavity was an additional BCP of 100  $\mu$ m and more thorough rinsing. At this point, we became confident that the major factor that influences the low-field  $Q_0$  is a good clean surface, i.e., free from chemical residues, contaminants and/or defects.

## 6 TEMPERATURE AND X-RAY MAPPING SYSTEM

As mentioned earlier, many cavities have suffered field emission with X-ray radiations. To localize emitter locations and the loss distributions in the cavity when it heats up or quenches, we started fabricating a temperature and X-ray mapping system. The detailed design and the mechanism were described in [5]. The first system was completed in August 2001 and tested with LANL cavity in August. Figures 9 and 10 show the pictures when the sensors were attached on the cavity. This is a rotating-arm type mapper with a drum on which 170 conductor strips were made on five Kapton films for electrical brush contacts.

Unfortunately, we had a lot of difficulties in fitting the sensor boards since we did not know the fact that the distances between cells on LANL cavity were very different from nominal distances that were used for designing the sensor boards. Also, we had a timing



problem in taking the data. All in all, it was a failure as a test and we are in the process of modifying the system based on the lessons learned from this test.



Figure 9: Temperature and X-ray sensors attached on the  $\beta=0.64$ , 700-MHz, 5-cell cavity.

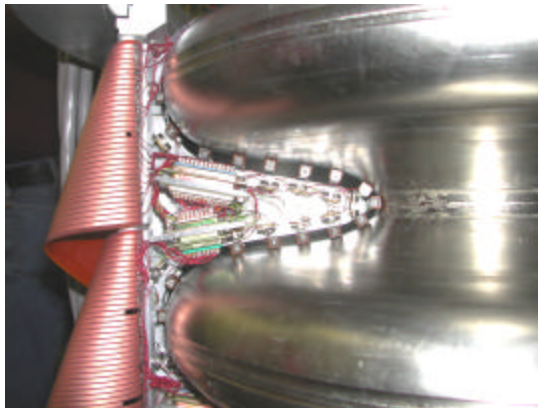


Figure 10: Temperature sensors (carbon resistors) and X-ray sensors (PIN diodes) attached on the cavity.

## 7 FUTURE PLANS

To meet increasing demands of higher gradients and higher  $Q_0$  values for cost reduction, we are planning to continue researches to establish the best way to produce cavities that show good results reliably. Our next goal will be  $Q_0 = 1 \times 10^{10}$  at  $E_{acc} = 11$  MV/m and  $E_{acc, max} = 15$  MV/m, which corresponds to  $E_{peak} = 51$  MV/m and  $H_{peak} = 1044$  Oe. This effort will include investigations to identify the cause(s) of field emission and other defects with temperature and X-ray mapping followed by detailed inspection of the cavity surface.

In parallel with this, we will try to determine the limitations of further BCP and helium processing in terms of achievable gradients. Moreover, if possible, we will try to use some other techniques such as electro-polishing and ozonated water rinsing to compare the results.

## 7 SUMMARY

The performance of all the six prototype APT 700-MHz 5-cell cavities is presented. All the cavities exceeded the APT requirements with ample margin assuring reliable operation. The achievement of these results with relatively large 5-cell cavities (surface area =  $0.858 \text{ m}^2$ ) and without high-temperature heat treatment ( $> 150^\circ\text{C}$ ) is remarkable.

For the future accelerators such as Accelerator-Driven Test Facility for AAA, however, the goals will be  $Q_0 = 1 \times 10^{10}$  at  $E_{acc} = 11$  MV/m. To achieve this goal with enough margin for reliable operation, we will have to solve the field emission problem and establish a technology to reach a maximum field of 15 MV/m and keep high  $Q_0$  values reliably.

## 8 REFERENCES

- [1] P. Lisowski, "The Accelerator Production of Tritium," Proc. PAC'97, Vancouver, B. C., Canada, May 1997, p. 3780.
- [2] T. Tajima et al., "Developments of 700-MHz 5-Cell Superconducting Cavities for APT," PAC2001, Chicago, Illinois, June 18-22, 2001.  
<http://laacg1.lanl.gov/scrflab/pubs/APT/LA-UR-01-3140.pdf>
- [3] J. L. Anderson, "Technology Development for the Accelerator Production of Tritium," PAC'99, New York, Mar. 29 - Apr. 2, 1999.
- [4] T. Tajima, et al., "Results of Vertical Tests with 700 MHz 5-cell ( $\beta=0.64$ ) Superconducting Cavities Developed for APT," Superconducting Proton Linac Workshop, Saclay, France, October 17-19, 2000 <http://laacg1.lanl.gov/scrflab/pubs/APT/la-ur-00-4949.pdf>
- [5] T. Tajima et al., "A New Temperature and X-ray Mapping System for 700-MHz 5-cell Superconducting Cavities," PAC2001, Chicago, Illinois, USA, June 18-22, 2001.  
<http://laacg1.lanl.gov/scrflab/pubs/APT/LA-UR-01-3163.pdf>
- [6] P. Balleyguier, "External Q Studies for APT SC-Cavity Couplers," *ibid.* [14], p. 133.
- [7] F. L. Krawczyk, "Summary of the APT Cavity Data – An Update,"  
<http://laacg1.lanl.gov/scrflab/pubs/APT/11-00-076.pdf>
- [8] H. Padamsee et al., "RF Superconductivity for Accelerators," p. 8, John Wiley & Sons, Inc. 1998.